Colloids and Surfaces A: Physicochemical and Engineering Aspects

Hydrogen peroxide-responsive micellar transition from spherical to worm-like in cetyltrimethylammonium bromide/3-fluorophenylboronic acid/fructose system

Ryotaro Miki,* Tsutomu Yamaki, Masaki Uchida, Hideshi Natsume

Faculty of Pharmacy and Pharmaceutical Sciences, Josai University, 1-1 Keyakidai, Sakado, Saitama 350-0295, Japan

**To whom correspondence should be addressed: Faculty of Pharmacy and Pharmaceutical Sciences, Josai University, 1-1 Keyakidai, Sakado, Saitama 350-0295, Japan*

E-mail: rmiki@josai.ac.jp

Tel: +81-49-271-7052

Fax: +81-49-271-7052

KEYWORDS: Hydrogen peroxide-responsive, phenylboronic acid, smart material, viscosity change, worm-like micelles

Highlights

• A novel hydrogen peroxide (H_2O_2)-responsive micellar system was prepared.

• The viscosity of the micellar system drastically increased depending on the H_2O_2 concentration.

• Cetyltrimethylammonium-bromide-based worm-like micelles are formed by adding 3-fluorophenol.

• 3-Fluorophenylboronate-fructose ester reacts with H_2O_2 to convert 3-fluorophenol.

ABSTRACT

In this study, we successfully prepared a novel hydrogen peroxide (H_2O_2)-responsive micellar system, whose viscosity drastically changes depending on H_2O_2 levels. The cationic surfactant cetyltrimethylammonium bromide (CTAB)/3-fluorophenol (3FPhOH) and CTAB/3-fluorophenylboronic acid (3FPBA) systems exhibited high viscosity. The viscosity of the CTAB/3FPBA system significantly decreased with the addition of fructose (Fru). The zero-shear viscosity of the CTAB/3FPBA/Fru system with 40 mM H_2O_2 increased 4×10^4-fold in comparison to that without H_2O_2. We confirmed that both the CTAB/3FPhOH and CTAB/3FPBA/Fru

with H_2O_2 systems form worm-like micelle (WLM) structures based on their rheological properties. The results of dynamic light scattering measurements supported the micellar transition with the addition of H_2O_2. We successfully demonstrated H_2O_2-responsive micellar transition from spherical/shorter rod-like micelles to long WLMs. We utilized the two reactions in the CTAB-based micellar system to control micellar transitions and viscosities: (i) Phenylboronic acid (PBA) forms a reversible cyclic ester structure with Fru and (ii) PBA reacts with H_2O_2 to convert phenol.

1. Introduction

Recently, smart materials, whose viscoelasticity changes in response to external stimuli, have garnered increasing attention. In particular, smart hydrogel can be used in drug delivery systems, analytical chemistry, and cell engineering [1–3]. Viscoelastic materials are categorized into two main types: those based on polymers and those self-assembled by low molecules.

Worm-like micelles (WLMs) are viscoelastic materials composed of small molecules. Spherical micelles grow into rod- and worm-like structures under appropriate conditions. Although the viscosities of spherical micelle solutions are low,

those of WLMs are high owing to their entanglement. WLMs exhibit unique viscoelasticity, which follows the Maxwell model with a single relaxation time (τ) [4,5]. External stimuli-responsive smart WLMs that respond to diol compounds [6–8], pH shifts [9,10], temperature shifts [11,12], light [13–16], redox [17,18] and CO_2 [19] have been reported and have potential for wide applications [20].

Phenylboronic acid (PBA) or PBA derivatives have been used in WLMs, whose viscosity changes with the addition of diol compounds such as fructose (Fru) or glucose (Glc) [6–8]. The hydroxyl group coordinates with PBA under basic conditions and PBA reversibly reacts with diol compounds to form a cyclic ester structure (Fig. 1a) [21]. Utilizing this response property, extensive research has been conducted on Glc-responsive drug release systems [22], sialic-acid-targeted materials for diagnosis/treatment [23], and Glc sensors [24,25]. In addition, PBA reacts with hydrogen peroxide (H_2O_2) to convert it to phenol and boric acid (Fig. 1b).

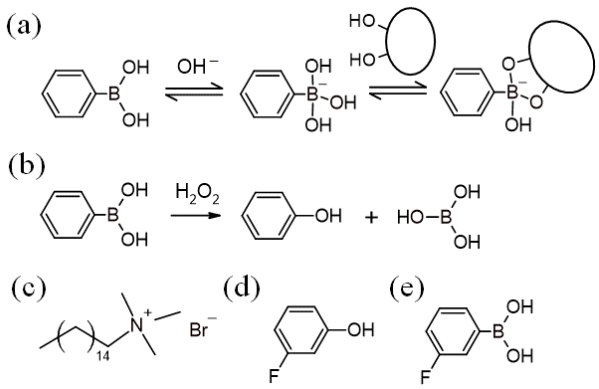

Fig. 1. (a) Acid–base equilibrium of PBA, and the cyclic boronate ester formation with

diol compounds. (b) Reaction scheme of PBA with H_2O_2. Chemical structures of (c) cetyltrimethylammonium bromide, (d) 3-fluorophenol, and (e) 3-fluorophenylboronic acid.

Owing to the reactive nature of PBA and H_2O_2, there have been several studies on the imaging/quantitative analysis of H_2O_2 [26,27], stimulus-responsive hydrogels [28–30] and multi-layer films [31]. H_2O_2-responsive WLMs have the potential for wide-field applications. However, to the best of our knowledge, H_2O_2-responsive WLMs have not been reported.

The cationic surfactant cetyltrimethylammonium bromide (CTAB, Fig. 1c) is a typical material used in WLMs [20]. Spherical micelles composed of CTAB were transformed into WLMs by adding appropriate aromatic compounds [20]. Adding phenol or phenol derivatives to the CTAB solution induces the transition from spherical micelles to WLMs [32–34]. We expect that by adding H_2O_2 to the CTAB/PBA system, PBA would be converted to phenol, which led to transformation of the micellar structure. However, because PBA is moderately similar to phenol in terms of its chemical structure and physicochemical properties, it cannot induce drastic micellar transitions. In addition, adding Fru to CTAB/PBA WLMs shortens and decreases their

viscosity [7].

In this study, we attempted to prepare a novel H_2O_2-responsive micellar system whose viscosity drastically increases depending on H_2O_2. We utilized the two reactions in the CTAB-based micellar system to control micellar transitions and viscosities: (i) PBA forms a reversible cyclic ester structure with Fru, and (ii) PBA reacts with H_2O_2 to convert phenol.

2. Materials and methods

2.1. Materials

CTAB, Fru, hydrochloric acid solution (1 mol/L), sodium hydroxide solution (1 and 8 mol/L), sodium dihydrogen phosphate, disodium hydrogen phosphate, sodium periodate ($NaIO_4$), L-ascorbic acid (Asc), sodium chloride (NaCl), and H_2O_2 aqueous solution (30%) were obtained from FUJIFILM Wako Pure Chemical Co., Osaka, Japan. 3-Fluorophenol (3FPhOH, Fig. 1d) and 3-fluorophenylboronic acid (3FPBA, Fig. 1e) were obtained from the Tokyo Chemical Industry (Tokyo, Japan). Glc and glycine (Gly) were obtained from Sigma-Aldrich (Tokyo, Japan).

2.2. Preparation of systems

We used 0.6 M phosphate buffer (pH 7.4) to prepare micellar samples. In the case of 0.1 M CTAB/50 mM 3FPBA/0.2 M Fru/0.6 M phosphate buffer (pH 7.4), the pH was adjusted to 7.3 using sodium hydroxide solution because forming of 3FPBA/Fru-ester promoted dissociation of 3FPBA and led to a lower pH. The prepared mixed micellar systems were stored at 25 °C for more than 24 h after mixing. Samples containing H_2O_2 were mixed to react sufficiently for more than 24 h before storage.

2.3. Observation of appearance

We prepared solutions (1.5 mL) in 6 mL glass vials. Images were captured 10 s after vials were inverted.

2.4. Rheological measurements

A stress-controlled rotational rheometer (MCR-102, Anton Paar, Ostfildern, Germany) with a cone plate or concentric cylinder was used for steady and dynamic rheological measurements at 25 °C. For the dynamic viscoelasticity measurements, we fixed the strain (γ) at 10%.

2.5. Foaming studies

We studied the foaming behavior of the micellar systems by referring to previous reports [35,36]. Six milliliters of the micellar solutions were placed in 20 mL vials with a stirrer bar. The samples were vigorously agitated using a magnetic stirrer (F-202H; Tokyo Garasu Kikai, Tokyo, Japan) at room temperature. Subsequently, the samples were stored at 25 °C, and observations and measurements of foam height were conducted.

2.6. Particle size measurements

We used a dynamic light scattering (DLS) instrument (Malvern Zetasizer Pro system, Malvern Panalytical, London, UK) equipped with a 4 mW and 633 nm HeNe laser at 25 °C for particle size measurements.

2.7. Ultraviolet (UV) spectroscopy

A UV spectrophotometer (UVmini-1240, Shimadzu, Kyoto, Japan) was used to measure the absorbance of 0.2 mM 3FPhOH at 282 nm to determine the pK_a of 3FPhOH. For the UV absorbance measurement, we used hydrochloric acid solution or sodium hydroxide solution to change the pH.

3. Results and discussion

3.1. Visual appearance of micellar systems

We combined 3FPBA and 3FPhOH in a CTAB-based micellar system. 3FPBA was converted to 3FPhOH to react with H_2O_2. We fixed the CTAB concentration at 0.1 M to prepare each micellar system using 0.6 M phosphate buffer (pH 7.4) as a solvent. We defined 0.1 M CTAB/50 mM 3FPBA system and 0.1 M CTAB/50 mM 3FPBA/0.2 M Fru system as system BA and system Fr, respectively. The appearance of the samples is shown in Fig. 2.

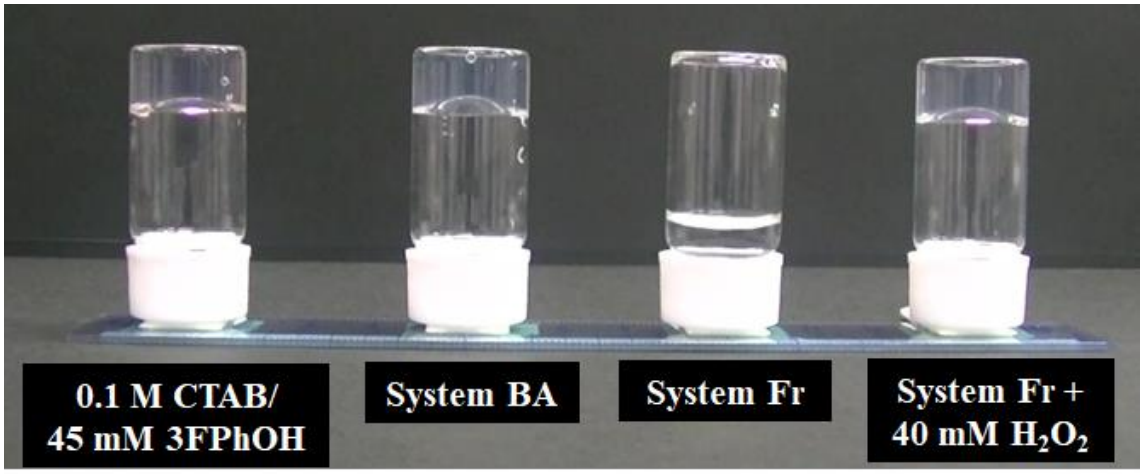

Fig. 2. Visual appearance of 0.1 M CTAB/45 mM 3FPhOH, system BA, system Fr, and system Fr with 40 mM H_2O_2.

The appearances of 0.1 M CTAB/45 mM 3FPhOH and system Fr with 40 mM H_2O_2

were pastel magenta and transparent, respectively. The color of pastel magenta was derived from 3FPhOH. The systems BA and Fr were colorless and transparent. The samples of 0.1 M CTAB/45 mM 3FPhOH, system BA, and system Fr with 40 mM H_2O_2 did not drop in inverted vials after 10 s, and they appeared gel-like (Fig. 2). However, system Fr rapidly dropped in inverted vials.

3.2. Steady-state viscosity measurements

We measured the steady-state viscosity to obtain the rheological relationship between the viscosity (η) and shear rate ($\dot{\gamma}$) (Fig. 3).

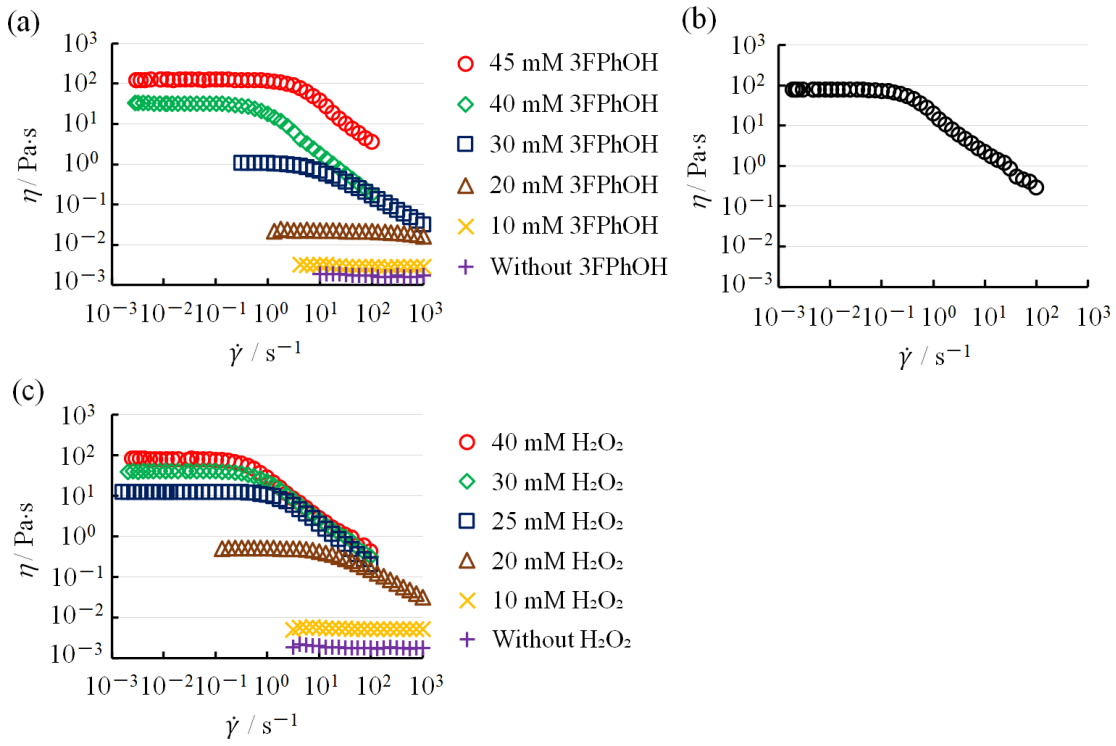

Fig. 3. Relationship between viscosity (η) and shear rate ($\dot{\gamma}$) in (a) 0.1 M CTAB/3FPhOH, (b) system BA, and (c) system Fr with H_2O_2.

Samples of 0.1 M CTAB/45 mM 3FPhOH, system BA, and system Fr with 40 mM H_2O_2 exhibited higher η (132.1, 80.0, and 77.8 Pa·s, respectively) at lower $\dot{\gamma}$. Moreover, η decreased depending on the value of $\dot{\gamma}$ at more than 0.14 s^{-1} for 0.1 M CTAB/45 mM 3FPhOH, 0.17 s^{-1} for system BA, and 0.25 s^{-1} for system Fr with 40 mM H_2O_2. A constant higher η indicates that when slower shear loads are applied to the system, the structure of the system recovers rapidly. Typical WLMs have a unique rheological property [37,38]. We employed the zero-shear viscosity (η_0) as an index of η by extrapolating η onto the y-axis, which is constant at a lower $\dot{\gamma}$. The η_0 of system BA and system Fr without H_2O_2 were 80.0 Pa·s and 2.0 mPa·s, respectively (Fig. 3b and c). The η_0 of system BA significantly decreased to 1/40,000 after adding 0.2 M Fru. This result is consistent with a previous study [7], where Fru was effective in decreasing the viscosity of CTAB/3FPBA micellar systems. In 0.1 M CTAB/3FPhOH, η_0 increased with increasing 3FPhOH concentration, η_0 of 45 mM 3FPhOH increased from 2.5 mPa·s to 132.1 Pa·s, and this was a 5×10^4-fold increase in comparison to the solution without 3FPhOH (Fig. 4a). In system Fr, η_0 increased with increasing H_2O_2

concentration, η_0 of 40 mM H_2O_2 increased from 2.0 mPa·s to 77.8 Pa·s, and this was a 4×10^4-fold increase in comparison to the solution without H_2O_2 (Fig. 4b). To demonstrate the selectivity of H_2O_2, we used $NaIO_4$ (oxidant), Asc (antioxidant agent), Glc (diol compound), Gly (amino acid), and NaCl (salt) as control additives for Fr. The values of η_0 after the addition of additives at the concentration of 20 mM or 40 mM were similar to those without H_2O_2 (1.7–2.7 mPa·s) (Fig. 4c). Thus, it was successfully demonstrated that the viscosity of system Fr can be increased without using any control additives in relation to that with H_2O_2.

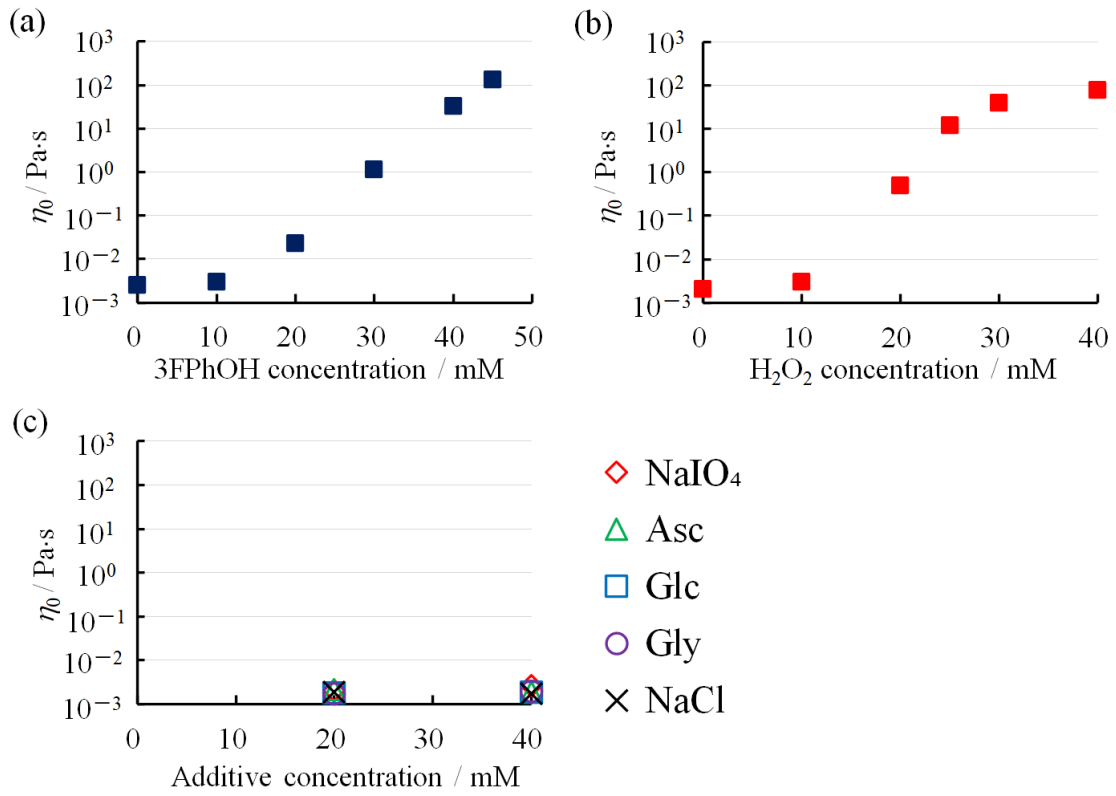

Fig. 4. (a) Relationship between η_0 and 3FPhOH concentration in 0.1 M CTAB/

3FPhOH, (b) relationship between η_0 and H_2O_2 concentration in system Fr with H_2O_2, and (c) relationship between η_0 and additive concentration in system Fr with additives.

3.3. Dynamic viscoelastic measurements

Dynamic viscoelastic measurements were performed to obtain additional rheological features. Both the storage (G') and loss moduli (G'') were obtained at varying frequencies (ω). These parameters are based on the Maxwell model expressed in Eqs. 1 and 2, respectively, as follows:

$$G' = \frac{\omega^2\tau^2}{1+\omega^2\tau^2} \cdot G_0 \qquad (1),$$

$$G'' = \frac{\omega\tau}{1+\omega^2\tau^2} \cdot G_0 \qquad (2),$$

where G_0 denotes the plateau modulus.

We obtained ω_c, which denotes the intersection of G' and G'', and obtained τ according to the following relation [38]:

$$\tau = \frac{1}{\omega_c} \qquad (3).$$

The relationship between G' and G'' at the same ω is known as the Cole–Cole plot. If the rheological character explains the Maxwell model with a single τ, a perfect semicircular curve is observed in the Cole–Cole plot, as expressed in Eq. 4 [4,39].

$$\left(G' - \frac{G_0}{2}\right)^2 + G''^2 = \frac{G_0^2}{4} \qquad (4).$$

In both 0.1 M CTAB/45 mM 3FPhOH and system Fr with 40 mM H_2O_2, G' was less than G'' at a low ω, but higher at a high ω, and G' fitted well to the Maxwell model (Fig. 5). This demonstrates that the liquid-like property is stronger in the lower ω region, and the gel-like property is stronger in the higher ω region. In contrast, in both the 0.1 M CTAB/30 mM 3FPhOH and system Fr with 20 mM H_2O_2, G' was less than G'' at a low ω, but slightly higher at a high ω, and G' and G'' did not adequately fit the Maxwell model (Fig. 5). Because the difference between G' and G'' is insignificant at a higher value of ω, the liquid-like property is generally stronger.

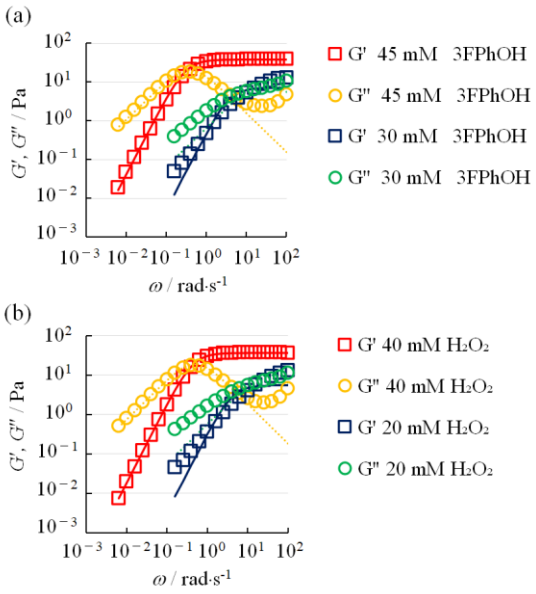

Fig. 5. Relationship between frequency and G' or G'' in (a) 0.1 M CTAB/3FPhOH and (b) system Fr with H_2O_2. The solid and dotted lines represent the curve-fittings according to Eqs. 1 and 2, respectively.

Because typical WLMs have a unique rheological character, which is the drawing of a perfect semicircular curve in the Cole–Cole plot, semicircular plotting in the Cole–Cole plot is one of the methods used to confirm the structure of WLMs [4,37,40]. Although the plotting was not semicircular in 0.1 M CTAB/30 mM 3FPhOH, as the concentration of 3FPhOH increased, the semicircle was almost perfect, and a perfect semicircular curve was obtained in 45 mM 3FPhOH (Fig. 6a).

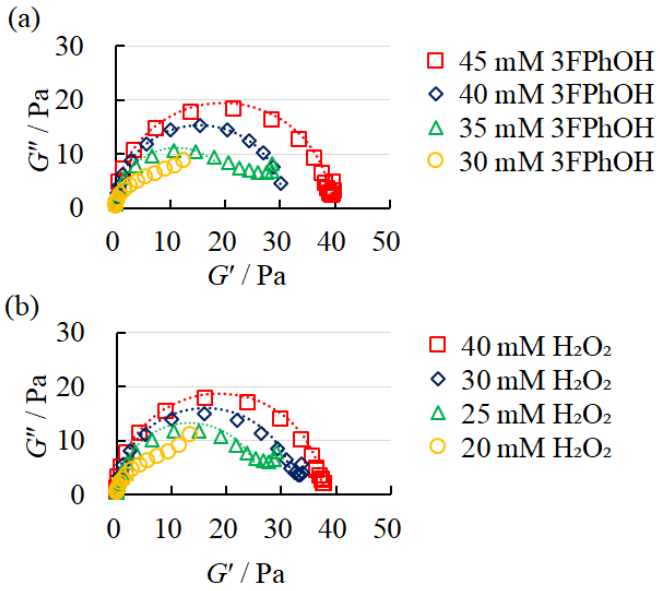

Fig. 6. Cole–Cole plot of (a) 0.1 M CTAB/3FPhOH and (b) system Fr with H_2O_2. The dotted lines represent the curve-fittings from Eq. 4.

In the system Fr with 20 mM H_2O_2, the semicircle was clearly absent. However, the semicircle became almost perfect with increasing H_2O_2, and a perfect semicircle was

observed in system Fr with 40 mM H_2O_2 (Fig. 6b). It was demonstrated that WLMs structures are formed in 0.1 M CTAB/45 mM 3FPhOH and system Fr with 40 mM H_2O_2. Considering that the addition of phenol or phenol derivatives into the CTAB solution induces a transition from spherical micelles to WLMs [32–34], these findings are acceptable.

We discuss the growth of WLMs based on their dynamic viscoelastic properties. The value of τ determined from Eq. 3 is an indicator of the entanglement of WLMs, and an increase in τ indicates the entanglement of WLMs [37,41]. The value of τ increased with the increase in 3FPhOH from 0.01 to 3.13 s in 0.1 M CTAB/3FPhOH (Fig. 7a). Similarly, the value of τ increased with the increase of H_2O_2 from 0.05 to 2.21 s in system Fr with H_2O_2 (Fig. 7b). These results indicate that an increase in 3FPhOH or H_2O_2 induces the elongation of WLMs in 0.1 M CTAB/3FPhOH and system Fr with H_2O_2.

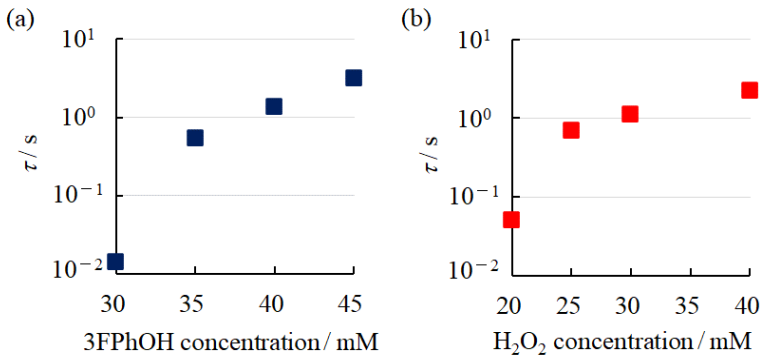

Fig. 7. (a) Relationship between relaxation time (τ) and 3FPhOH concentration in 0.1 M CTAB/3FPhOH. (b) Relationship between τ and H_2O_2 concentration in system Fr with H_2O_2.

3.4. Foaming behavior

The surfactant system is likely to generate and stabilize the foam. Understanding the foaming behavior of micellar systems is useful for several applications in cosmetics, personal care products, and oil recovery. We examined the foaming behavior of system Fr with H_2O_2 (Fig. 8).

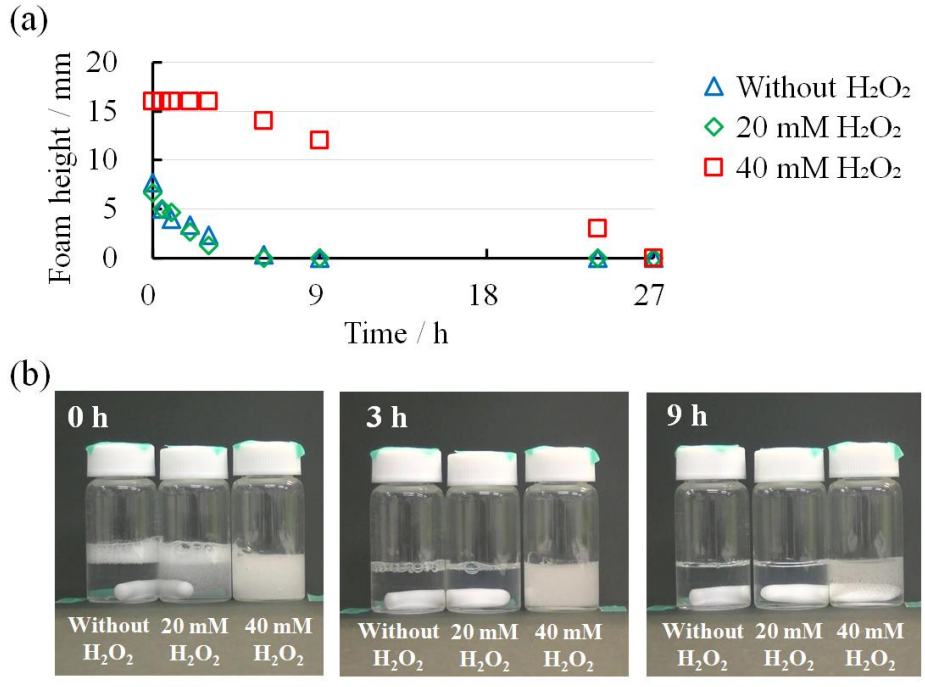

Fig. 8. (a) Relationship between time and foam height in system Fr with H_2O_2, (b)

Visual appearance showing changes of foam height with time in system Fr with 40 mM H_2O_2. The height of the glass vial was 57 mm.

In both the samples without H_2O_2 and with 20 mM H_2O_2, the foam height started to decrease from approximately 7 mm at 0.5 h and continued to decrease to 0 mm over 9 h. However, in the samples with 40 mM H_2O_2, the foam height was constant until 3 h, and then continued to decrease slowly over 27 h.

3.5. DLS measurements

DLS measurements support the evaluation of micellar shape variations [6,19,42–44]. DLS measurements were performed to study the micellar transition upon addition of 3FPhOH or H_2O_2. In 0.1 M CTAB/3FPhOH, the size distributions shifted to larger sizes with increasing 3FPhOH (Fig. 9a). The mean particle size (Z-average) of 0.1 M CTAB without 3FPhOH was 8.0 nm (Fig. 9b). This indicates that spherical micelles are formed in 0.1 M CTAB/3FPhOH [43,44].

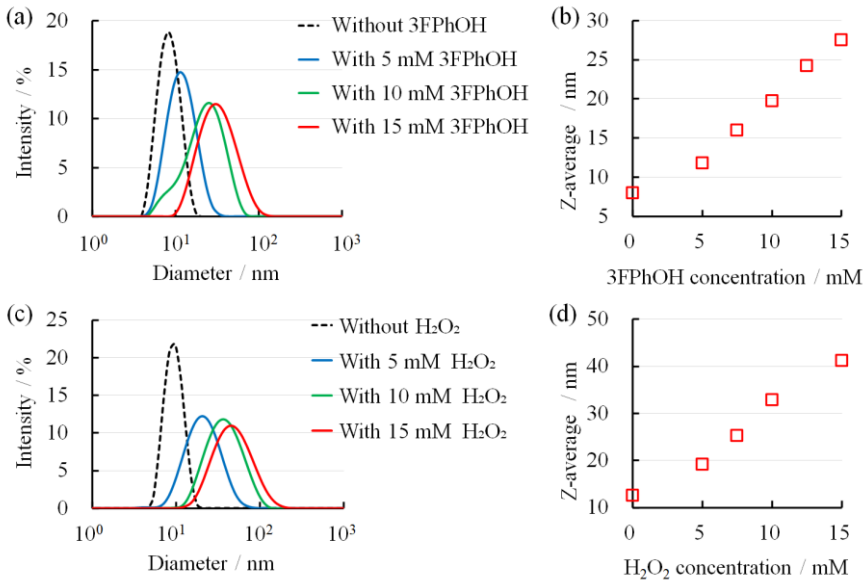

Fig. 9. (a) Size distributions in 0.1 M CTAB/3FPhOH. (b) Relationship between 3FPhOH concentration and Z-average in 0.1 M CTAB/3FPhOH. (c) Size distributions in 0.1 M CTAB/20 mM 3FPBA/0.5 M Fru with H_2O_2. (d) Relationship between H_2O_2 concentration and Z-average in 0.1 M CTAB/20 mM 3FPBA/0.5 M Fru with H_2O_2.

The Z-average increased with increasing 3FPhOH from 8.0 to 27.6 nm (Fig. 9b). This demonstrates that the micellar transition from spherical micelles to rod-like micelles was induced by the addition of 3FPhOH into the CTAB system. In 0.1 M CTAB/20 mM 3FPBA/0.5 M Fru with H_2O_2, the size distributions also shifted to larger sizes with an increase in H_2O_2 (Fig. 9c). The Z-average of 0.1 M CTAB/20 mM 3FPBA/0.5 M Fru without H_2O_2 was 12.6 nm, which was slightly greater than that of 0.1 M CTAB without 3FPhOH (Fig. 9d). It demonstrates that spherical micelles or shorter rod-like micelles

are formed in 0.1 M CTAB/20 mM 3FPBA/0.5 M Fru system [43,44]. The Z-average increased with increasing H_2O_2 from 12.6 to 41.2 nm (Fig. 9d). This result indicates that rod-like micelles elongated with the addition of H_2O_2, which supports the results of the increase in the value of η_0 in system Fr with H_2O_2 (Fig. 4b).

3.6. UV spectroscopy

To study the ionized state of 3FPhOH at pH 7.4, we investigated the pK_a of 3FPhOH through UV spectrophotometry. The relationship between pH and absorbance at 282 nm of 0.2 mM 3FPhOH is shown in Fig. 10.

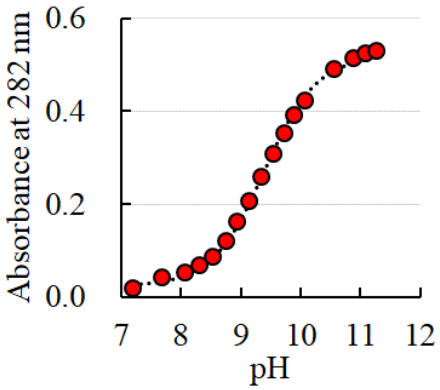

Fig. 10. Absorbance at 282 nm of 0.2 mM 3FPhOH at varying pH values.

From the absorbance profile, the pK_a of 3FPhOH was determined as 9.39. This value is reasonable because a previous study reported a pK_a value of 9.28 [45]. The pK_a obtained indicates that 3FPhOH mainly exists in a molecular form at pH 7.4.

3.7. Mechanisms of micellar transition

The presumed mechanisms of micellar transition are shown in Fig. 11.

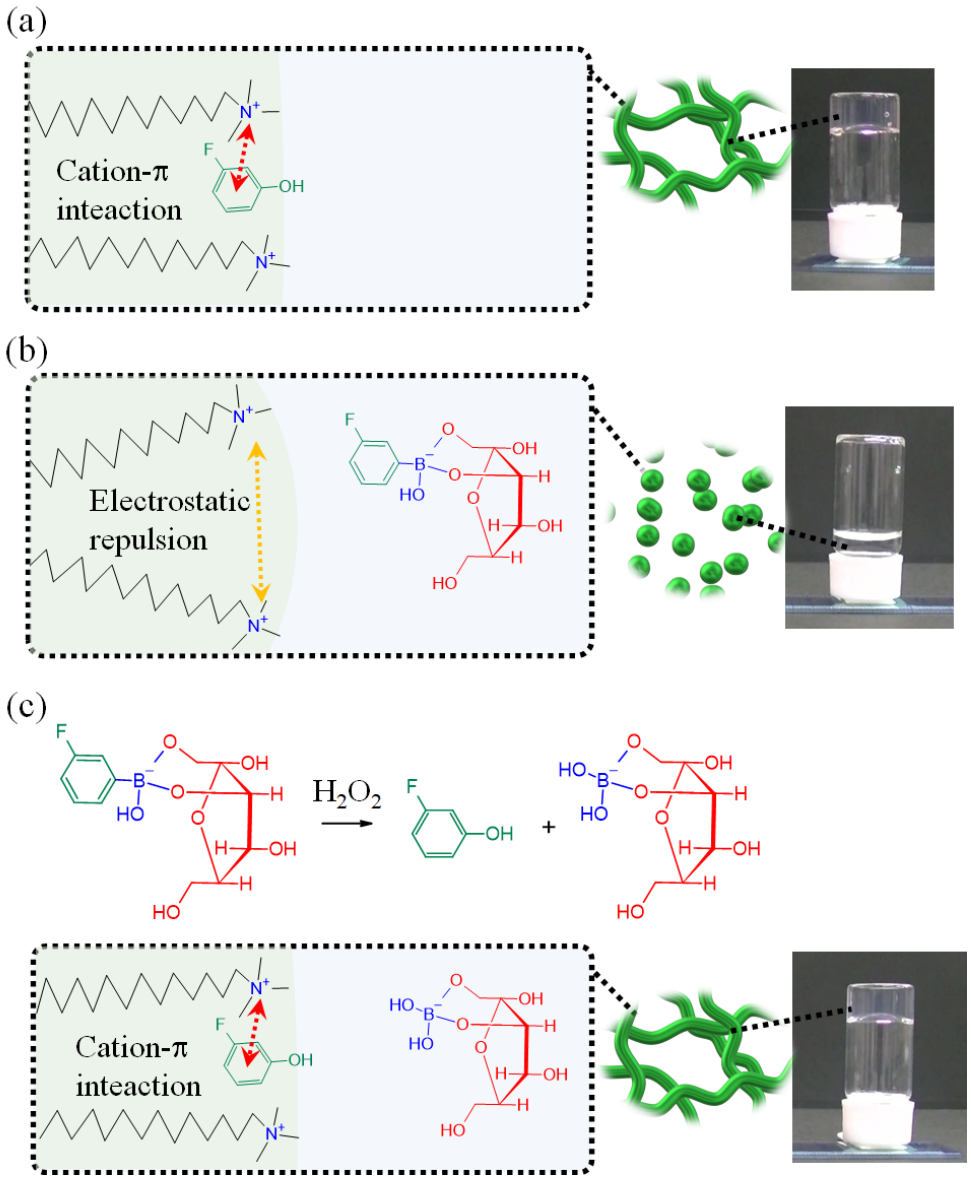

Fig. 11. Presumed mechanisms of micellar transition in (a) 0.1 M CTAB/3FPhOH, (b) system Fr, and (c) system Fr with H_2O_2.

3FPhOH mainly exists in molecular form at pH 7.4 in 0.1 M CTAB/3FPhOH because the pK_a of 3FPhOH is 9.39. Therefore, it is considered that there is no significant effect of electrostatic interaction between the 3-fluorophenoxide-anion and the quaternary ammonium groups of CTAB. The cation–π interactions between the quaternary ammonium ion of CTAB and the benzene ring of aromatic compounds have been studied through ^{1}H NMR [46–48] and ^{19}F NMR spectroscopy [7,8,49]. The occurrence of these interactions is confirmed by the upfield shifts for methyl or methylene groups around the quaternary ammonium groups of CTAB when aromatic compounds coexist in ^{1}H NMR. These shifts are attributed to an increase in the electron density around the quaternary ammonium groups of CTAB owing to the interacting benzene ring of aromatic compounds. However, in ^{19}F NMR, the occurrence of these interactions can be confirmed by downfield shifts of the ^{19}F signal of fluorobenzene derivatives upon the addition of CTAB. This shift is due to the decrease in the electron density near the aromatic ring owing to the interacting quaternary ammonium groups of CTAB. Numerous aromatic compounds that interact with CTAB have been reported, including sodium salicylate [47], benzoic acid [48], and PBA derivatives [7]. Therefore, the generality of the cation–π interactions between CTAB and aromatic compounds is high [48]. The aromatic ring of phenol or phenol derivatives also interacts with the

quaternary ammonium groups of CTAB via cation–π interactions [46,50,51]. Thus, it is presumed that the quaternary ammonium groups of CTAB also interact with the aromatic ring of 3FPhOH via cation-π interaction in 0.1 M CTAB/3FPhOH (Fig. 11a). The cation-π interaction weakens the electrostatic repulsion between the head groups of CTAB. This tightens the packing of CTAB, and the packing state becomes appropriate for WLMs, which induces micellar transformation from spherical to worm-like structures [16,18,40].

In system Fr, Fru forms a cyclic ester with 3FPBA that does not interact with CTAB and exists in the bulk aqueous layer [7] (Fig. 11b). Therefore, the electrostatic repulsion among the head groups of CTAB was stronger than that of CTAB/3FPhOH. This changes the packing state of CTAB, which is appropriate for spherical/shorter rod-like micelles. Consequently, spherical/shorter rod-like micelles that exhibited low viscosity were formed.

In system Fr with H_2O_2, 3FPBA in the 3FPBA/Fru ester is converted to 3FPhOH after the addition of H_2O_2 (Fig. 11c). This led to an increase in the amount of 3FPhOH that interacts with CTAB. Thus, the electrostatic repulsion between the head groups of CTAB weakened. This tightened the packing state of CTAB resulting in a transformation from spherical/shorter rod-like micelles to long WLMs. The generation

of adequate amounts of 3FPhOH by adding H_2O_2 resulted in a high viscosity. Cleaved boric acid from the 3FPBA/Fru ester exists in the bulk aqueous layer as a Fru-ester or free-form that does not interact with CTAB.

4. Conclusions

We successfully demonstrated H_2O_2-responsive micellar transition from spherical/shorter rod-like micelles to long WLMs whose viscosity drastically increases. This study proposed a unique system to control micellar transitions and viscosities by utilizing two operating principles of PBA: (i) PBA forms a reversible cyclic ester structure with Fru and (ii) PBA reacts with H_2O_2 to convert phenol. In the proposed micellar system, 3FPBA in the 3FPBA/Fru ester converts to 3FPhOH by reacting with H_2O_2, and the resulting 3FPhOH interacts with CTAB. This conversion induces a micellar transition from spherical/shorter rod-like micelles to long WLMs.

References

[1] M. Vázquez-González, I. Willner, Stimuli-responsive biomolecule-based hydrogels and their applications, Angew. Chemie Int. Ed. 59 (2020) 15342–15377. https://doi.org/10.1002/ANIE.201907670.

[2] K. Zhang, Q. Feng, Z. Fang, L. Gu, L. Bian, Structurally dynamic hydrogels for biomedical applications: Pursuing a fine balance between macroscopic stability and microscopic dynamics, Chem. Rev. 121 (2021) 11149–11193.

https://doi.org/10.1021/acs.chemrev.1c00071.
[3] X. Du, J. Zhou, J. Shi, B. Xu, Supramolecular hydrogelators and hydrogels: From soft matter to molecular biomaterials, Chem. Rev. 115 (2015) 13165–13307. https://doi.org/10.1021/acs.chemrev.5b00299.
[4] T. Shikata, H. Hirata, T. Kotaka, Micelle formation of detergent molecules in aqueous media: Viscoelastic properties of aqueous cetyltrimethylammonium bromide solutions, Langmuir. 3 (1987) 1081–1086. https://doi.org/10.1021/la00078a035.
[5] T. Shikata, H. Hirata, T. Kotaka, Micelle formation of detergent molecules in aqueous media. 2. Role of free salicylate ions on viscoelastic properties of aqueous cetyltrimethylammonium bromide-sodium salicylate solutions, Langmuir. 4 (1988) 354–359. https://doi.org/10.1021/la00080a019.
[6] R. Miki, C. Takei, Y. Ohtani, K. Kawashima, A. Yoshida, Y. Kojima, Y. Egawa, T. Seki, D. Iohara, M. Anraku, F. Hirayama, K. Uekama, Glucose responsive rheological change and drug release from a novel worm-like micelle gel formed in cetyltrimethylammonium bromide/phenylboronic acid/water system, Mol. Pharm. 15 (2018) 1097–1104. https://doi.org/10.1021/acs.molpharmaceut.7b00988.
[7] R. Miki, T. Yamauchi, K. Kawashima, Y. Egawa, T. Seki, Multinuclear NMR study on the formation and polyol-induced deformation mechanisms of wormlike micelles composed of cetyltrimethylammonium bromide and 3-fluorophenylboronic acid, Langmuir. 37 (2021) 3438–3445. https://doi.org/10.1021/acs.langmuir.1c00103.
[8] R. Miki, T. Yamaki, M. Uchida, H. Natsume, Diol responsive viscosity increase in a cetyltrimethylammonium bromide/sodium salicylate/3-fluorophenylboronic acid micelle system, RSC Adv. 12 (2022) 6668–6675. https://doi.org/10.1039/D1RA08831A.
[9] Y. Lin, X. Han, J. Huang, H. Fu, C. Yu, A facile route to design pH-responsive viscoelastic wormlike micelles: Smart use of hydrotropes, J. Colloid Interface Sci. 330 (2009) 449–455. https://doi.org/10.1016/j.jcis.2008.10.071.
[10] Y. Feng, Z. Chu, pH-Tunable wormlike micelles based on an ultra-long-chain “pseudo” gemini surfactant, Soft Matter. 11 (2015) 4614–4620. https://doi.org/10.1039/c5sm00677e.
[11] T.S. Davies, A.M. Ketner, S.R. Raghavan, Self-assembly of surfactant vesicles that transform into viscoelastic wormlike micelles upon heating, J. Am. Chem. Soc. 128 (2006) 6669–6675. https://doi.org/10.1021/ja060021e.

[12] Y. Lin, Y. Qiao, Y. Yan, J. Huang, Thermo-responsive viscoelastic wormlike micelle to elastic hydrogel transition in dual-component systems, Soft Matter. 5 (2009) 3047–3053. https://doi.org/10.1039/b906960g.

[13] H. Sakai, Y. Orihara, H. Kodashima, A. Matsumura, T. Ohkubo, K. Tsuchiya, M. Abe, Photoinduced reversible change of fluid viscosity, J. Am. Chem. Soc. 127 (2005) 13454–13455. https://doi.org/10.1021/ja053323+.

[14] A.M. Ketner, R. Kumar, T.S. Davies, P.W. Elder, S.R. Raghavan, A simple class of photorheological fluids: Surfactant solutions with viscosity tunable by light, J. Am. Chem. Soc. 129 (2007) 1553–1559. https://doi.org/10.1021/ja065053g.

[15] M. Akamatsu, M. Shiina, R.G. Shrestha, K. Sakai, M. Abe, H. Sakai, Photoinduced viscosity control of lecithin-based reverse wormlike micellar systems using azobenzene derivatives, RSC Adv. 8 (2018) 23742–23747. https://doi.org/10.1039/c8ra04690e.

[16] Y. Tu, Q. Chen, Y. Shang, H. Teng, H. Liu, Photoresponsive behavior of wormlike micelles constructed by gemini surfactant 12-3-12·2Br$^-$ and different cinnamate derivatives, Langmuir. 35 (2019) 4634–4645. https://doi.org/10.1021/acs.langmuir.8b04290.

[17] K. Tsuchiya, Y. Orihara, Y. Kondo, N. Yoshino, T. Ohkubo, H. Sakai, M. Abe, Control of viscoelasticity using redox reaction, J. Am. Chem. Soc. 126 (2004) 12282–12283. https://doi.org/10.1021/ja0467162.

[18] J. Sugai, N. Saito, Y. Takahashi, Y. Kondo, Synthesis and viscoelastic properties of gemini surfactants containing redox-active ferrocenyl groups, Colloids Surf. A Physicochem. Eng. Asp. 572 (2019) 197–202. https://doi.org/10.1016/j.colsurfa.2019.04.010.

[19] X. Su, M.F. Cunningham, P.G. Jessop, Switchable viscosity triggered by CO_2 using smart worm-like micelles, Chem. Commun. 49 (2013) 2655–2657. https://doi.org/10.1039/c3cc37816k.

[20] Z. Chu, C.A. Dreiss, Y. Feng, Smart wormlike micelles, Chem. Soc. Rev. 42 (2013) 7174–7203. https://doi.org/10.1039/c3cs35490c.

[21] G. Springsteen, B. Wang, A detailed examination of boronic acid–diol complexation, Tetrahedron. 58 (2002) 5291–5300. https://doi.org/10.1016/S0040-4020(02)00489-1.

[22] J. Wang, Z. Wang, J. Yu, A.R. Kahkoska, J.B. Buse, Z. Gu, Glucose-responsive insulin and delivery systems: Innovation and translation, Adv. Mater. 32 (2020) 1902004. https://doi.org/10.1002/adma.201902004.

[23] M. Sanjoh, Y. Miyahara, K. Kataoka, A. Matsumoto, Phenylboronic acids-based diagnostic and therapeutic applications, Anal. Sci. 30 (2014) 111–117. https://doi.org/10.2116/analsci.30.111.

[24] X. Sun, B.M. Chapin, P. Metola, B. Collins, B. Wang, T.D. James, E. V. Anslyn, The mechanisms of boronate ester formation and fluorescent turn-on in ortho-aminomethylphenylboronic acids, Nat. Chem. 11 (2019) 768–778. https://doi.org/10.1038/s41557-019-0314-x.

[25] X. Sun, T.D. James, Glucose sensing in supramolecular chemistry, Chem. Rev. 115 (2015) 8001–8037. https://doi.org/10.1021/cr500562m.

[26] A.R. Lippert, G.C. Van de Bittner, C.J. Chang, Boronate oxidation as a bioorthogonal reaction approach for studying the chemistry of hydrogen peroxide in living systems, Acc. Chem. Res. 44 (2011) 793–804. https://doi.org/10.1021/AR200126T.

[27] L. Wu, A.C. Sedgwick, X. Sun, S.D. Bull, X.P. He, T.D. James, Reaction-based fluorescent probes for the detection and imaging of reactive oxygen, nitrogen, and sulfur species, Acc. Chem. Res. 52 (2019) 2582–2597. https://doi.org/10.1021/acs.accounts.9b00302.

[28] M. Ikeda, T. Tanida, T. Yoshii, I. Hamachi, Rational molecular design of stimulus-responsive supramolecular hydrogels based on dipeptides, Adv. Mater. 23 (2011) 2819–2822. https://doi.org/10.1002/adma.201004658.

[29] M. Ikeda, T. Tanida, T. Yoshii, K. Kurotani, S. Onogi, K. Urayama, I. Hamachi, Installing logic-gate responses to a variety of biological substances in supramolecular hydrogel-enzyme hybrids., Nat. Chem. 6 (2014) 511–518. https://doi.org/10.1038/nchem.1937.

[30] M. Zhang, C.C. Song, F.S. Du, Z.C. Li, Supersensitive oxidation-responsive biodegradable PEG hydrogels for glucose-triggered insulin delivery, ACS Appl. Mater. Interfaces. 9 (2017) 25905–25914. https://doi.org/10.1021/ACSAMI.7B08372.

[31] K. Sato, M. Takahashi, M. Ito, E. Abe, J.I. Anzai, H_2O_2-induced decomposition of layer-by-layer films consisting of phenylboronic acid-bearing poly(allylamine) and poly(vinyl alcohol), Langmuir. 30 (2014) 9247–9250. https://doi.org/10.1021/la501750s.

[32] D. Varade, C. Rodríguez-Abreu, J.G. Delgado, K. Aramaki, Viscoelasticity and mass transfer in phenol–CTAB aqueous systems, Colloid Polym. Sci. 285 (2007) 1741–1747. https://doi.org/10.1007/S00396-007-1761-2.

[33] M. Singh, C. Ford, V. Agarwal, G. Fritz, A. Bose, V.T. John, G.L. McPherson,

Structural evolution in cationic micelles upon incorporation of a polar organic dopant, Langmuir. 20 (2004) 9931–9937. https://doi.org/10.1021/la048967u.

[34] V. Agarwal, M. Singh, G. McPherson, V. John, A. Bose, Microstructure evolution in aqueous solutions of cetyl trimethylammonium bromide (CTAB) and phenol derivatives, Colloids Surf. A Physicochem. Eng. Asp. 281 (2006) 246–253. https://doi.org/10.1016/j.colsurfa.2006.02.047.

[35] K. Yu, H. Zhang, C. Hodges, S. Biggs, Z. Xu, O.J. Cayre, D. Harbottle, Foaming Behavior of Polymer-Coated Colloids: The Need for Thick Liquid Films, Langmuir. 33 (2017) 6528–6539. https://doi.org/10.1021/acs.langmuir.7b00723.

[36] C. Da, X. Chen, J. Zhu, S. Alzobaidi, G. Garg, K.P. Johnston, Elastic gas/water interface for highly stable foams with modified anionic silica nanoparticles and a like-charged surfactant, J. Colloid Interface Sci. 608 (2022) 1401–1413. https://doi.org/10.1016/j.jcis.2021.10.058.

[37] R.G. Shrestha, L.K. Shrestha, K. Aramaki, Formation of wormlike micelle in a mixed amino-acid based anionic surfactant and cationic surfactant systems, J. Colloid Interface Sci. 311 (2007) 276–284. https://doi.org/10.1016/j.jcis.2007.02.050.

[38] D. Varade, S.C. Sharma, K. Aramaki, Viscoelastic behavior of surfactants worm-like micellar solution in the presence of alkanolamide, J. Colloid Interface Sci. 313 (2007) 680–685. https://doi.org/10.1016/j.jcis.2007.04.065.

[39] A. Khatory, F. Lequeux, F. Kern, S.J. Candau, Linear and nonlinear viscoelasticity of semidilute solutions of wormlike micelles at high salt content, Langmuir. 9 (1993) 1456–1464. https://doi.org/10.1021/la00030a005.

[40] J. Li, M. Zhao, H. Zhou, H. Gao, L. Zheng, Photo-induced transformation of wormlike micelles to spherical micelles in aqueous solution, Soft Matter. 8 (2012) 7858–7864. https://doi.org/10.1039/c2sm25218j.

[41] K. Hashizaki, H. Taguchi, Y. Saito, A novel reverse worm-like micelle from a lecithin/sucrose fatty acid ester/oil system, Colloid Polym. Sci. 287 (2009) 1099–1105. https://doi.org/10.1007/s00396-009-2076-2.

[42] L. Rose J, B.V.R. Tata, V.K. Aswal, P.A. Hassan, Y. Talmon, L. Sreejith, pH-switchable structural evolution in aqueous surfactant-aromatic dibasic acid system, Eur. Phys. J. E. 38 (2015) 1–9. https://doi.org/10.1140/epje/i2015-15004-9.

[43] W. Kang, X. Hou, P. Wang, Y. Zhao, T. Zhu, C. Chen, H. Yang, Study on the effect of the organic acid structure on the rheological behavior and aggregate transformation of a pH-responsive wormlike micelle system, Soft Matter. 15

(2019) 3160–3167. https://doi.org/10.1039/C9SM00088G.

[44] S.J. Mushi, W. Kang, H. Yang, Z. Li, K. Ibrashev, M. Issakhov, P.E. Mabeyo, Effect of aromatic acid on the rheological behaviors and microstructural mechanism of wormlike micelles in betaine surfactant, J. Mol. Liq. 332 (2021) 115908. https://doi.org/10.1016/j.molliq.2021.115908.

[45] M.D. Liptak, K.C. Gross, P.G. Seybold, S. Feldgus, G.C. Shields, Absolute pK_a determinations for substituted phenols, J. Am. Chem. Soc. 124 (2002) 6421–6427. https://doi.org/10.1021/ja012474j.

[46] P. Sabatino, A. Szczygiel, D. Sinnaeve, M. Hakimhashemi, H. Saveyn, J.C. Martins, P. Van der Meeren, NMR study of the influence of pH on phenol sorption in cationic CTAB micellar solutions, Colloids Surf. A Physicochem. Eng. Asp. 370 (2010) 42–48. https://doi.org/10.1016/j.colsurfa.2010.08.042.

[47] X.L. Wei, A.L. Ping, P.P. Du, J. Liu, D.Z. Sun, Q.F. Zhang, H.G. Hao, H.J. Yu, Formation and properties of wormlike micelles in solutions of a cationic surfactant with a 2-hydroxypropoxy insertion group, Soft Matter. 9 (2013) 8454–8463. https://doi.org/10.1039/c3sm51017d.

[48] S. Kumar, D. Sharma, D. Kabir, Role of partitioning site in producing viscoelasticity in micellar solutions, J. Surfactants Deterg. 8 (2005) 247–252. https://doi.org/10.1007/s11743-005-0353-3.

[49] M. Vermathen, P. Stiles, S.J. Bachofer, U. Simonis, Investigations of monofluoro-substituted benzoates at the tetradecyltrimethylammonium micellar interface, Langmuir. 18 (2002) 1030–1042. https://doi.org/10.1021/la0109765.

[50] J.P. Mata, V.K. Aswal, P.A. Hassan, P. Bahadur, A phenol-induced structural transition in aqueous cetyltrimethylammonium bromide solution, J. Colloid Interface Sci. 299 (2006) 910–915. https://doi.org/10.1016/J.JCIS.2006.02.032.

[51] R. Chaghi, L.C. de Ménorval, C. Charnay, G. Derrien, J. Zajac, Interactions of phenol with cationic micelles of hexadecyltrimethylammonium bromide studied by titration calorimetry, conductimetry, and ^{1}H NMR in the range of low additive and surfactant concentrations, J. Colloid Interface Sci. 326 (2008) 227–234. https://doi.org/10.1016/j.jcis.2008.07.035.